

Remote control of LTI systems over networks with state quantization*

Hideaki Ishii^a and Tamer Başar^b

^aDepartment of Information Physics and Computing
University of Tokyo, Tokyo, Japan.
E-mail: hideaki_ishii@ipc.i.u-tokyo.ac.jp

^bCoordinated Science Laboratory
University of Illinois, Urbana, IL, U.S.A.
Email: tbasar@control.csl.uiuc.edu

Abstract

We consider a remote control system, where the plant and the controller are connected by a network cable, and study the problem of designing quantizers for its stabilization. It is assumed that the computation available on the plant side in the sensor/actuator is limited and also that broadcast of messages is allowed over the channel.

Keywords: Data rate limitation, Quantization, Remote control, Sampled-data systems, Stabilizability.

1 Introduction

Quantization effects are present in most control systems, as they heavily rely on digital components, and have long been studied. Recently, such effects that arise in systems with networks have received considerable attention. When a digital network is present in a feedback system, quantization levels determine the data rate for the transmission of control related signals and hence the cost for communication. While quantization levels may not be the largest factor contributing to high data rates [8], careful design of communication is mandatory in large-scale systems, which certainly involves coding aspects.

This viewpoint has prompted studies on design methods for quantizers efficient in terms of data rate. In particular, stabilization problems for LTI systems with one quantizer are considered in, e.g., [1–3, 5–7, 9–14]. In these problems, the communication over the channel is in one direction, and signals are sent from the sensor side directly to the actuator side. Hence, only one quantizer, or coder, is present. The minimum data rates are derived for such problems for deterministic cases in [3, 9, 12, 13] and for stochastic cases in [10, 11]; these minimum rates can be achieved through the use of quantizers that are time varying and require memory on both the coders and the decoders.

In this paper, we study quantization issues in a remote control system, as depicted in Fig. 1. This is another realistic setup in the context of control over networks. Here, the plant and

*This research was supported by NSF Grant CCR 00-85917 ITR. Corresponding author: Hideaki Ishii

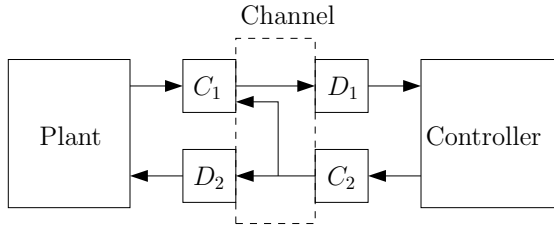


Figure 1: Remote control system with coders C_i and decoders D_i , $i = 1, 2$

the controller are physically distant, and the sensor and the actuator are connected to the controller over a shared network. The sensor output is encoded in the coder C_1 , transmitted over the channel, and then decoded at the decoder D_1 on the controller side. Similarly, the controller output is sent over the channel to the actuator through the coder C_2 and the decoder D_2 . The setup is more complicated than the one mentioned above, and clearly there are two quantizers. Here, our focus is on problems related to quantization, and thus we ignore the issue of time delay. This assumption may be justified, e.g., when remote control takes place in a short distance where no delay due to queuing in routers is present. For example, in an automobile engine, the controller is separately located to avoid heat and vibration.

Specifically, we develop a design method for the two quantizers to achieve stabilization of the overall system and to use the data rate efficiently. We employ time-invariant, memoryless quantizers and, in particular, those of the logarithmic type. In [2], such quantizers were first considered and were shown to be the “coarsest” type under a certain optimization problem for stabilization of discrete-time systems. Logarithmic quantizers were also studied in a sampled-data setup in [6], where the emphasis was on quadratic stability in the continuous time domain. Here too, logarithmic quantizers were shown to be more efficient over other quantizers such as the uniform ones. In this paper, we follow this approach of [6] for the remote control problem, which involves its extension to a state quantization problem.

One of the objectives of the study is to characterize the tradeoffs in communication arising in this setup. One is between the rates in the two directions of communication (to and from the controller). We find that, to maintain stability, a lower rate in one direction may result in a higher rate in the other. Another tradeoff is between the data rate and the performance with respect to the degree of stability. That is, more data rate implies that the state of the system decays faster, and vice versa.

In the design method, we incorporate several features of remote control. It is natural that the computation available in the coder and the decoder on the plant side is very limited, and thus most computation takes place in the controller. This aspect is modeled by the use of time-invariant, memoryless quantizers. We note however that minimum data rates as in [3, 9, 12, 13] seem difficult to obtain for this class of quantizers. This is mainly because the designs usually rely on the Lyapunov methods, as we shall see in our development; see [13] for more discussion.

We also make use of the broadcast feature in the network, which allows multiple nodes to receive a single message at the same time without extra data rate. We examine the case where the controller transmits messages to both C_1 and D_2 as in Fig. 1.

This paper is organized as follows. In Section 2, we give the definition of quantizers used throughout the paper. In Section 3, we state our problem of remote control over networks. This problem motivates us to study in Section 4 a state quantization problem formulated as an extension of the quantization methods in [6]. The results will be applied to solving the remote control problem in Section 5.

2 Quantizers

We first give the definition of quantizers [6]. Given n bounded intervals $\mathcal{A}_j \subset \mathbb{R}$, $j = 1, 2, \dots, n$, we say the set $\mathcal{A}_1 \times \dots \times \mathcal{A}_n \subset \mathbb{R}^n$ is a bounded *rectangle*.

Definition 2.1 A *partition* $\{\mathcal{Q}_j\}_{j \in \mathcal{S}}$ of \mathbb{R}^n is a set of bounded rectangles with a countable *index set* $\mathcal{S} = \mathbb{Z}_+$ such that (i) $\mathcal{Q}_i \cap \mathcal{Q}_j = \emptyset$, $i \neq j$, and $\cup_{j \in \mathcal{S}} \mathcal{Q}_j = \mathbb{R}^n$, (ii) $0 \in \mathcal{Q}_0$, and (iii) for $j \neq 0$, $0 \notin \text{cl}(\mathcal{Q}_j)$. Given a partition $\{\mathcal{Q}_j\}_{j \in \mathcal{S}}$, and a countable set of points in \mathbb{R}^n , $\{q_j\}_{j \in \mathcal{S}}$ with $q_0 = 0$, a *quantizer* $Q : \mathbb{R}^n \rightarrow \{q_j\}_{j \in \mathcal{S}}$ is defined by $Q(x) = q_j$ if $x \in \mathcal{Q}_j$, $j \in \mathcal{S}$.

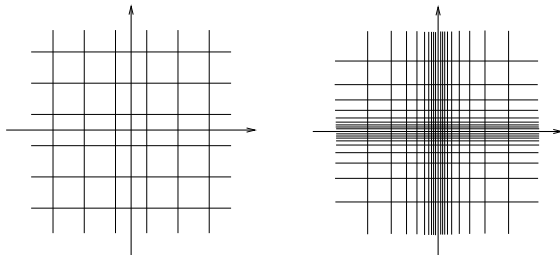


Figure 2: Uniform (left) and logarithmic (right) partitions

The quantizers used in this paper will be time invariant and memoryless. One simple and commonly used quantizer class is that of *uniform quantizers*. They employ the uniform partitioning of \mathbb{R}^n : Given $\Delta > 0$, let the index set be $\mathcal{S} = \mathbb{Z}^n$ and the partition cells be $\mathcal{Q}_{[j_1 \dots j_n]} = \prod_{l=1}^n [(j_l - 1/2)\Delta, (j_l + 1/2)\Delta)$ (see Fig. 2).

Another class is that of *logarithmic quantizers* [2]. Let us first introduce the following notation for intervals in \mathbb{R} : For $s \in \{-1, 0, 1\}$ and $0 \leq a < b$, $s[a, b) \subset \mathbb{R}$ is defined as

$$s[a, b) := \begin{cases} (-b, -a], & \text{if } s = -1, \\ \{0\}, & \text{if } s = 0, \\ [a, b), & \text{if } s = 1. \end{cases}$$

The logarithmic partition on \mathbb{R}^n is defined as follows. Given $\delta > 1$, take the index set as $\mathcal{S} = \mathbb{Z}^n \times \{-1, 0, 1\}^n$. For $[j_1 \dots j_n s_1 \dots s_n] \in \mathcal{S}$, set the cells as $\mathcal{Q}_{[j_1 \dots j_n s_1 \dots s_n]} = \prod_{l=1}^n s_l[\delta^{j_l}, \delta^{j_l+1})$; see Fig. 2. The partitioning in logarithmic quantizers is efficient in communication for the control objective of stability; unlike the uniform partition, the cells are finer around the origin, where more precise information is needed, and the cells far from the origin are coarser¹.

¹Note that in this definition, the origin itself is a cell; as a result, in contrast to the uniform quantizers, asymptotic stability can be achieved, as we will see later.

3 Remote control problem

We now formulate the remote control problem addressed in this paper. Consider the system depicted in Fig. 3. The triple (A, B, C) ² represents the continuous-time LTI plant given by the state equations

$$\begin{aligned}\dot{x}(t) &= Ax(t) + Bu(t), \\ y(t) &= Cx(t),\end{aligned}$$

where $x(t) \in \mathbb{R}^n$ is the state, $u(t) \in \mathbb{R}^m$ is the control input, and $y(t) \in \mathbb{R}^p$ is the output. It is assumed that $A \neq 0$ and $\text{rank } B = m$, and that (A, B) is stabilizable and (C, A) detectable. Thus, we can design a state feedback gain $K \in \mathbb{R}^{m \times n}$ and an estimator gain $L \in \mathbb{R}^{n \times p}$ such that the matrices $A + BK$ and $A + LC$ are Hurwitz. On the remote site is mainly the state observer; it outputs the estimated state $\hat{x}(t)$. We give its state equation shortly. As mentioned earlier, we assume that there is no time delay in the communication.

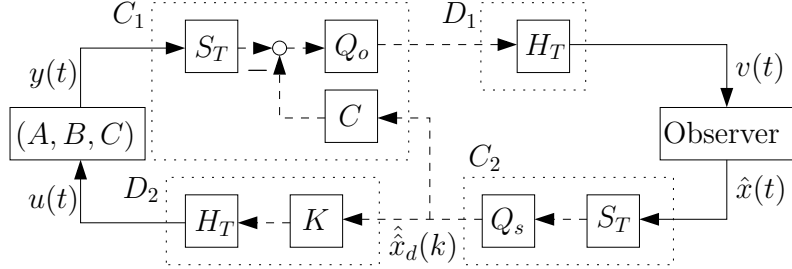


Figure 3: Remote control system

The signals transmitted over the channel are in discrete time with sampling period T (assuming the presence of synchronized clocks) and are quantized. In the coder C_2 , the estimated state $\hat{x}(t)$ is sampled by a uniform sampler $S_T : \hat{x} \mapsto \hat{x}_d$, $\hat{x}_d(k) = \hat{x}(kT)$, $k \in \mathbb{Z}_+$, and then quantized by a quantizer Q_s on \mathbb{R}^n , as defined in Section 2; we call Q_s the *state quantizer* and denote its output by $\hat{x}_d(k)$. In the decoder D_2 , the quantized signal $\hat{x}_d(k)$ is used for the control input $u(t)$; K is the stabilizing feedback gain and H_T is the zeroth order hold given by $H_T : u_d \mapsto u$, $u(t) = u_d(k)$, $t \in [kT, (k+1)T)$, $k \in \mathbb{Z}_+$.

The same quantized signal $\hat{x}_d(k)$ is also received by the coder C_1 , where the innovation process $y(kT) - C\hat{x}_d(k)$ is calculated. The innovation is quantized by the *output quantizer* Q_o on \mathbb{R}^p and then transmitted to the decoder D_1 containing a hold.

The observer has the state equation

$$\dot{\hat{x}}(t) = A\hat{x}(t) + Bu(t) - Lv(t) + LC \left(\hat{x}(kT) - \hat{x}_d(k) \right) \quad (1)$$

for $t \in [kT, (k+1)T)$, $k \in \mathbb{Z}_+$, where $\hat{x}(t) \in \mathbb{R}^n$ is the estimated state and $v(t) = Q_o(y(kT) - C\hat{x}_d(k)) \in \mathbb{R}^p$ is the quantized innovation. It has a standard structure except for the last term, which is the error from the state quantization; this term essentially cancels $\hat{x}_d(k)$ used in the innovation and replace it with the usual $\hat{x}(kT)$. We note that this error and also $u(t)$ are

²Here we follow the conventional notation; C is a matrix and not a coder.

available on the observer side, though not indicated in the figure for simplicity. The initial state is fixed to $\hat{x}(0) = 0$. Let the estimation error be $e(t) := x(t) - \hat{x}(t)$.

We are now in a position to state our *remote control problem*. Given a state feedback gain K and an estimator gain L , design the quantizers Q_o and Q_s and the sampling period T such that the closed-loop system is asymptotically stable; that is, $x(t) \rightarrow 0$ and $e(t) \rightarrow 0$ as $t \rightarrow \infty$.

We have several remarks. As discussed in Section 1, remote control arises in systems that have little computation capability in the sensors and actuators. In Fig. 3, the computation required in C_1 and D_2 is small in the following sense. By definition, the output of the state quantizer Q_s takes a discrete value, say, q_j , $j \in \mathcal{S}$. What is sent over the channel is the index j . In C_1 and D_2 , we need decoders that map j to Cq_j and Kq_j , respectively; these values are calculated off-line. Thus, it is emphasized that there is no matrix multiplication on the plant side; most on-line computation is carried out in the observer.

In Fig. 3, $\hat{x}(k)$ is broadcast by C_2 and received by D_2 and C_1 . (Hence, C_1 does also decoding.) The motivation for this is as follows: In a controller/observer design problem, it is standard to design so that the estimation error e becomes small at a faster rate than the state x does. In doing so, if we were to quantize $y(kT)$, the quantization would have to be fine throughout the output space \mathbb{R}^p . This may be costly in terms of data rate. In our setup, it is the innovation $y(kT) - C\hat{x}_d(k)$ that is sent; the quantization needs to be fine only around the origin, and hence for Q_o , a logarithmic type quantizer can be used, which is efficient in data rate³.

In this paper, we take a two-stage design approach to solve this problem. In the first stage, the quantizers are constructed separately, Q_s via state feedback design and Q_o via observer design. The designs are based on the quantized control scheme studied in [6], and the stability criterion is in continuous time. In particular, existing methods are used for the output quantizer Q_o . In Section 4, the methodology is extended for the state quantizer Q_s . In the next stage, we tune the quantizers for the stability of the overall remote control system. Although the quantizer design methods deal with general quantizers as in the definition in Section 2, in the second stage, we limit the classes of quantizers to the logarithmic ones. The details of these two stages are described in Section 5.

4 Sampled-data control with state quantization

In this section, we give a design method for state quantizers.

4.1 Problem formulation

Consider the continuous-time LTI plant (A, B) given by the state equation

$$\dot{x}(t) = Ax(t) + Bu(t),$$

³The idea of quantizing innovations is also used in, e.g., [3, 9–11, 13]. There, the coder and the decoder share an auxiliary state which is updated based only on the quantized information; the innovation between this state and the actual state can be calculated in the coder alone. In contrast, in our scheme, the coder does not have memory, so the path from C_2 to C_1 is critical.

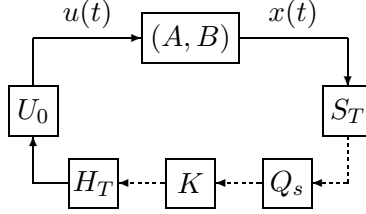


Figure 4: Quantized sampled-data system

where $x(t) \in \mathbb{R}^n$ is the state and $u(t) \in \mathbb{R}^m$ is the control input. Assume that $A \neq 0$ and $\text{rank} B = m$, and that (A, B) is stabilizable. The matrix $K \in \mathbb{R}^{m \times n}$ is a stabilizing state feedback gain. It is assumed to be LQR optimal: Given positive-definite matrices $Q \in \mathbb{R}^{n \times n}$ and $R \in \mathbb{R}^{m \times m}$, let $P_s \in \mathbb{R}^{n \times n}$ be the unique positive-definite solution of the Riccati equation

$$A'P_s + P_sA - P_sBR^{-1}B'P_s + Q = 0. \quad (2)$$

The LQR optimal gain is $K := -R^{-1}B'P_s$.

Let the *control Lyapunov function* be $V_s(x) := x'P_sx$, $x \in \mathbb{R}^n$, and $J_s := Q + P_sBR^{-1}B'P_s$. For every trajectory $x(\cdot)$ of the system, the decay rate of $V_s(x(t))$ (i.e., the rate at which $V_s(x(t))$ is guaranteed to decrease) is determined by J_s : The derivative of V_s along the trajectories is given by

$$\dot{V}_s(x, u) := (Ax + Bu)'P_sx + x'P_s(Ax + Bu). \quad (3)$$

With $u = Kx$ we have $\dot{V}_s(x, Kx) = -x'J_sx$. In this sense, this system is said to be *quadratically stable with respect to* (P_s, J_s) .

We turn our interest to the sampled-data system with a quantizer as in Fig. 4. This represents a simple setup where a digital channel connects the sensor and the actuator. We are interested in finding a large sampling period and a coarse quantizer while the closed-loop system maintains quadratic stability with a decay rate similar to that of the original continuous-time system.

Here, Q_s is a quantizer defined by a state partition $\{\mathcal{Q}_j\}_{j \in \mathcal{S}}$ and its output values $\{q_j\}_{j \in \mathcal{S}} \subset \mathbb{R}^n$. The matrix $U_0 \in \mathbb{R}^{m \times m}$ is an additional design parameter, which allows some freedom in the control values. We will see that the identity matrix is not the best choice in our scheme. Also, denote by $\mathcal{B}_x(r)$ the ball in \mathbb{R}^n with center x and radius r .

We give some stability definitions for the system. We say that, for the closed-loop system in Fig. 4, the ball $\mathcal{B}_0(r_0)$ is *attractive* if, for every $x(0) \in \mathbb{R}^n$, the trajectory $x(\cdot)$ converges to $\mathcal{B}_0(r_0)$. In particular, if there exists a positive-definite J such that every trajectory satisfies $\dot{V}_s(x(t), u(t)) \leq -x(t)'Jx(t)$ whenever $x(t) \notin \mathcal{B}_0(r_1)$ with $r_1 = r_0\sqrt{\lambda_{\min}(P_s)/\lambda_{\max}(P_s)}$, the ball $\mathcal{B}_0(r_0)$ is said to be *quadratically attractive with respect to* (P_s, J) . In the case with $r_0 = 0$, the closed-loop system is *quadratically stable with respect to* (P_s, J) .

The *state quantization problem* is as follows: Given $\epsilon \in (0, 1)$, find a sampling period T , a quantizer Q_s , and a matrix U_0 such that for some $r_0 \geq 0$, the ball $\mathcal{B}_0(r_0)$ is quadratically attractive with respect to $(P_s, \epsilon J_s)$ for the closed-loop system in Fig. 4.

We remark that this problem is an extension of the problems studied in [6, 7], where it is the signal $Kx(t)$ that is sampled and quantized. The dimension of the quantized signal is now n instead of m . The approach here is analogous to the one taken there. In this problem, the

parameter ϵ represents the degree of stability in terms of the decay rate. Sampled-data systems have a slower decay rate than that of the original continuous-time system. Moreover, we can show through examples that there is a tradeoff between ϵ and the data rate. Such examples are given in [6].

4.2 Control Lyapunov function approach

The design objective is to achieve quadratic stability with guaranteed decay rate for a fixed control Lyapunov function.

Fix $\epsilon \in (0, 1)$. For $u \in \mathbb{R}^m$, we denote by $\mathcal{X}(u)$ the set of states for which u decreases V_s :

$$\mathcal{X}(u) := \left\{ x \in \mathbb{R}^n : \dot{V}_s(x, u) \leq -\epsilon x' J_s x \right\}.$$

This set $\mathcal{X}(u)$ plays a crucial role in our design. By (2) and (3), this can be expressed as

$$\mathcal{X}(u) = \left\{ x \in \mathbb{R}^n : x' K' R [(1 + \epsilon) K x - 2u] \leq (1 - \epsilon) x' Q x \right\}.$$

Now to obtain a simpler expression for $\mathcal{X}(u)$, we introduce some assumptions and notation. First, we select $Q = 1/(1 - \epsilon)I$ without loss of generality. Let a subspace \mathcal{M} of \mathbb{R}^n be $\mathcal{M} := (\text{Ker}K)^\perp = \text{Im}K'$. Since $\text{rank}K = \text{rank}B = m$, we have $\dim\mathcal{M} = m$. Hence, there is an orthonormal basis $\{e_1, \dots, e_m\} \subset \mathbb{R}^n$ of \mathcal{M} . Let $E := [e_1 \ \dots \ e_m] \in \mathbb{R}^{n \times m}$. Since \mathcal{M} is a subspace, for every $x \in \mathbb{R}^n$, there are $\alpha \in \mathbb{R}^m$ and $y \in \mathcal{M}^\perp$ such that $x = E\alpha + y$. We use this decomposition extensively in the following development. Finally, let $S := (1 + \epsilon)E'K'RKE$.

With these notations and with $\|\cdot\|$ denoting the Euclidean norm, we obtain the following form for $\mathcal{X}(u)$: For $u \in \mathbb{R}^m$,

$$\mathcal{X}(u) = \left\{ E\alpha + y : \alpha \in \mathbb{R}^m, y \in \mathcal{M}^\perp, \alpha'(S - I)\alpha - 2\alpha'S[(1 + \epsilon)KE]^{-1}u \leq \|y\|^2 \right\}.$$

To further simplify its expression, we use $\tilde{B} := (1 + \epsilon)BKE$ and replace U_0 with $\tilde{U}_0 := (KE)^{-1}U_0KE/(1 + \epsilon)$. Also, let $u_j = \tilde{U}_0 E' q_j$, $j \in \mathcal{S}$. Notice that, if $x(kT) \in \mathcal{Q}_j$, then $u(t) = u_j$ for $t \in [kT, (k + 1)T)$, $k \in \mathbb{Z}_+$.

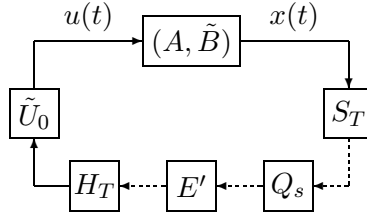


Figure 5: Equivalent system

A system equivalent to the one in Fig. 4, but using the newly defined variables \tilde{B} , \tilde{U}_0 , and E , is shown in Fig. 5. Then, for (A, \tilde{B}) , $\mathcal{X}(u)$ is

$$\mathcal{X}(u) = \left\{ E\alpha + y : \alpha \in \mathbb{R}^m, y \in \mathcal{M}^\perp, \alpha'(S - I)\alpha - 2\alpha'Su \leq \|y\|^2 \right\}. \quad (4)$$

We see in the expression above that the parameters α and $\|y\|$ are the essential components in the state space. Note that y is in the kernel space of K and is thus less relevant for control

compared to α . Assume that $S > I$. It then follows that, for a fixed $y \in \mathcal{M}^\perp$, the cross-section of $\mathcal{X}(u)$ is an ellipsoid with a center at $x = E(S - I)^{-1}Su + y$, as in (4).

A sufficient condition for the stability of the system is given by the following lemma.

Lemma 4.1 Suppose that the quantized sampled-data controller is designed so that there exists $r_1 \geq 0$ such that if $x(0) \in \mathcal{Q}_j$, $j \in \mathcal{S}$, then $x(t) \in \mathcal{X}(u_j) \cup \mathcal{B}_0(r_1)$ for $t \in [0, T]$. Then, for the closed-loop system in Fig. 4, $\mathcal{B}_0(r_0)$ is quadratically attractive with respect to $(P_s, \epsilon J_s)$, where

$$r_0 = r_1 \sqrt{\lambda_{\max}(P_s) / \lambda_{\min}(P_s)}. \quad (5)$$

Proof Denote the cell index which $x(kT)$ is in by $j_k \in \mathcal{S}$. Then, by the given hypothesis, $x(t) \in \mathcal{X}(u_{j_k}) \cup \mathcal{B}_0(r_1)$ for $t \in [kT, (k+1)T)$, $k \in \mathbb{Z}_+$. This means that at each $t \geq 0$ either the control Lyapunov function $V_s(x(t))$ is decreasing, by the definition of $\mathcal{X}(u_j)$, or else $x(t)$ is in $\mathcal{B}_0(r_1)$. The smallest level set of $V_s(\cdot)$ containing $\mathcal{B}_0(r_1)$ is $\mathcal{E}_0 = \{x \in \mathbb{R}^n : V_s(x) \leq \lambda_{\max}(P_s)r_1^2\}$. This is an invariant set, and hence $x(t)$ goes into and stays in \mathcal{E}_0 . Finally, the smallest ball that contains \mathcal{E}_0 is $\mathcal{B}_0(r_0)$. \square

The lemma shows that it is important to keep track of the state trajectories during one sampling period. We can derive a simple bound on the trajectories as follows.

For $T > 0$, let

$$c_T := \max_{t \in [0, T]} \|e^{At} - I\|, \quad d_T := \max_{t \in [0, T]} \left\| \int_0^t e^{A\tau} \tilde{B} d\tau \right\|.$$

Note that $c_T, d_T \rightarrow 0$ as $T \rightarrow 0$, and since $A \neq 0$, if $T > 0$, then $c_T > 0$.

Now, given $x_0 \in \mathbb{R}^n$ and $u \in \mathbb{R}^m$, define

$$\mathcal{G}_{x_0}(u) := \mathcal{B}_{x_0}(c_T \|x_0\| + d_T \|u\|). \quad (6)$$

This set serves as a simple bound on trajectories as shown below.

Lemma 4.2 Let $x(\cdot)$ be the trajectory starting at $x(0) = x_0$ with a constant control $u \in \mathbb{R}^m$. Then $x(t) \in \mathcal{G}_{x_0}(u)$ for $t \in [0, T]$.

Proof It easily follows that for $t \in [0, T]$

$$\begin{aligned} \|x(t) - x_0\| &= \left\| e^{At}x_0 + \int_0^t e^{A\tau} \tilde{B} d\tau u - x_0 \right\| \\ &\leq \|e^{At} - I\| \cdot \|x_0\| + \left\| \int_0^t e^{A\tau} \tilde{B} d\tau \right\| \cdot \|u\| \\ &\leq c_T \|x_0\| + d_T \|u\|. \end{aligned} \quad \square$$

4.3 Solution to the quantized sampled-data problem

The sampled-data problem with quantization is characterized in this section. First, the bound on trajectories in Lemma 4.2 can be used to obtain a simpler sufficient condition from Lemma 4.1.

Let $\mathcal{G}_j := \cup_{x_0 \in \mathcal{Q}_j} \mathcal{G}_{x_0}(u_j)$, $j \in \mathcal{S}$. This clearly gives a bound on the trajectories starting in \mathcal{Q}_j . Using this set, we can reduce the sufficient condition to the following one.

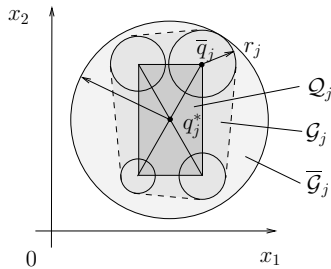


Figure 6: Sets \mathcal{G}_j and $\bar{\mathcal{G}}_j$

Proposition 4.3 Suppose that there exists $r_1 \geq 0$ such that $\mathcal{G}_j \subset \mathcal{X}(u_j) \cup \mathcal{B}_0(r_1)$ for $j \in \mathcal{S}$. Then, for the closed-loop system in Fig. 4, $\mathcal{B}_0(r_0)$ is quadratically attractive with respect to $(P_s, \epsilon J_s)$, where r_0 is as in (5).

Proof By the definition of \mathcal{G}_j , the condition implies that, for every $x(0) \in \mathcal{X}_j$, the trajectory of the system satisfies $x(t) \in \mathcal{X}(u_j) \cup \mathcal{B}_0(r_1)$ for $t \in [0, T]$. Thus, by Lemma 4.1, the ball $\mathcal{B}_0(r_0)$ is quadratically attractive. \square

The stabilization problem is now reduced to a countable set inclusion one. The difficulty that remains in the sufficient condition above is due to the complicated structure of the sets \mathcal{G}_j . Although \mathcal{G}_j is a union of balls, it is not a ball itself. We avoid dealing with this set by introducing a larger ball as follows. For the $n = 2$ case, the set \mathcal{G}_j can be roughly sketched as in Fig. 6. This set is a union of balls with the centers at $x_0 \in \mathcal{Q}_j$. Since the radii are proportional to $\|x_0\|$ and $\|u_j\|$, the largest ball is the one centered at the corner of \mathcal{Q}_j furthest from the origin. As a bound on \mathcal{G}_j , we can use a ball centered at the midpoint of the cell large enough to contain this ball.

Let

$$\bar{q}_j := \arg \sup \{\|x\| : x \in \mathcal{Q}_j\}, \quad \underline{q}_j := \arg \inf \{\|x\| : x \in \mathcal{Q}_j\}.$$

Since $0 \in \mathcal{Q}_0$, $\underline{q}_0 = 0$. Let $q_0^* = 0$, and for $j \neq 0$ let $q_j^* \in \mathbb{R}^m$ be the midpoint in \mathcal{Q}_j : $q_j^* := (\bar{q}_j + \underline{q}_j)/2$. Denote by r_j the radius of the ball $\mathcal{G}_{\bar{q}_j}(u_j)$; from (6), $r_j := c_T \|\bar{q}_j\| + d_T \|u_j\|$. Finally, let

$$\bar{\mathcal{G}}_j := \{x \in \mathbb{R}^n : \|x - q_j^*\| \leq \|\bar{q}_j - q_j^*\| + r_j\}. \quad (7)$$

Clearly,

$$\bar{\mathcal{G}}_j \supset \mathcal{G}_j, \quad (8)$$

and $\bar{\mathcal{G}}_j$ is a ball in \mathbb{R}^n with its center at $x = q_j^* = E\alpha_j^* + y_j^*$.

On the other hand, as mentioned above, the set $\mathcal{X}(u_j)$ has a cross-section for each $y \in \mathcal{M}^\perp$ of an ellipsoid with its center at $x = E(S - I)^{-1}Su_j + y$. Thus, to achieve the inclusion $\bar{\mathcal{G}}_j \subset \mathcal{X}(u_j)$, it is reasonable to have these centers coincide for each j , i.e., $q_j^* = E(S - I)^{-1}Su_j + y_j^*$. It is sufficient to have

$$\tilde{U}_0 = S^{-1}(S - I) \quad \text{and} \quad q_j = q_j^*.$$

Therefore, the quantizer's output q_j corresponding to the cell \mathcal{Q}_j is its center point. The use of $\bar{\mathcal{G}}_j$ instead of \mathcal{G}_j greatly simplifies the problem albeit at the expense of conservatism in T .

We are now in a position to construct a quantized sampled-data controller.

1. Fix $\epsilon \in (0, 1)$. Select matrices Q and R in (2) so that $S \geq 2I$ (the reason for using this condition, instead of $S > I$, is a rather technical one). There always exist such Q and R [6]. Set $\tilde{U}_0 = S^{-1}(S - I)$.
2. Given a state partition $\{\mathcal{Q}_j\}_{j \in \mathcal{S}}$, set $q_j = q_j^*$ for $j \in \mathcal{S}$.
3. Let $\mathcal{S}_0 := \{j \in \mathcal{S} : \|q_j\| \leq \sqrt{\sigma_1} \|\bar{q}_j - q_j\|\}$. Note that we always have $0 \in \mathcal{S}_0$. If \mathcal{S}_0 is finite, we can proceed with our design. For $j \in \mathcal{S} \setminus \mathcal{S}_0$, select, $T_j > 0$ small enough that

$$c_{T_j} < \frac{1}{\|\bar{q}_j\|} \left(\frac{1}{\sqrt{\sigma_1}} \|q_j\| - \|\bar{q}_j - q_j\| \right), \quad (9)$$

$$d_{T_j} \leq \frac{\sigma_m}{\sigma_m - 1} \sqrt{\left(\frac{\sigma_m - 1}{\sigma_1 - 1} - \frac{1}{\sigma_1} \right) \left[1 - \sigma_1 \left(\frac{\|\bar{q}_j - q_j\| + c_{T_j} \|\bar{q}_j\|}{\|q_j\|} \right)^2 \right]}, \quad (10)$$

where σ_1 and σ_m are the largest and the smallest eigenvalues of S . Set $T^* = \inf_{j \in \mathcal{S} \setminus \mathcal{S}_0} T_j$.

4. Take $T \geq T^*$ such that the set $\mathcal{S}_1 := \mathcal{S}_0 \cup \{j \in \mathcal{S} : T_j < T\}$ is finite. If such T exists, let

$$r_1 = \max_{j \in \mathcal{S}_1} \left[\|q_j\| + \|\bar{q}_j - q_j\| + c_T \|\bar{q}_j\| + d_T \left(1 - \frac{1}{\sigma_m} \right) \|\alpha_j\| \right]$$

$$\text{and } r_0 = r_1 \sqrt{\lambda_{\max}(P_s) / \lambda_{\min}(P_s)}.$$

We now have the main theorem for quantizers with $T > 0$.

Theorem 4.4 For the closed-loop system in Fig. 4 with the quantized sampled-data controller just defined, the ball $\mathcal{B}_0(r_0)$ is quadratically attractive with respect to $(P_s, \epsilon J_s)$.

Proof By Proposition 4.3 and (8), it is sufficient to show that $\bar{\mathcal{G}}_j \subset \mathcal{X}(u_j) \cup \mathcal{B}_0(r_1)$ for $j \in \mathcal{S}$. We prove this in two steps.

Step 1 For $j \in \mathcal{S} \setminus \mathcal{S}_1$, $\bar{\mathcal{G}}_j \subset \mathcal{X}(u_j)$.

Proof Fix $j \in \mathcal{S} \setminus \mathcal{S}_1$. Express q_j as $q_j = E\alpha_j + y_j$, where $\alpha_j \in \mathbb{R}^m$ and $y_j \in \mathcal{M}^\perp$. Let

$$\begin{aligned} \hat{r}_j &:= \|\bar{q}_j - q_j\| + r_j = \|\bar{q}_j - q_j\| + c_T \|\bar{q}_j\| + d_T \|u_j\|, \\ c_j(\beta) &:= \alpha_j'(S - I)\alpha_j + \beta^2, \quad \beta \in \mathbb{R}. \end{aligned}$$

Then, note that from (7)

$$\bar{\mathcal{G}}_j = \{x : \|x - q_j\| \leq \hat{r}_j\} = \{E\alpha + y : \|\alpha - \alpha_j\|^2 + \|y - y_j\|^2 \leq \hat{r}_j^2\}$$

since $E(\alpha - \alpha_j) \perp (y - y_j)$ and $E'E = I$, and that from (4)

$$\mathcal{X}(u_j) = \{E\alpha + y : (\alpha - \alpha_j)'(S - I)(\alpha - \alpha_j) \leq c_j(\|y\|)\}.$$

Given $y \in \mathcal{M}^\perp$ with $\|y - y_j\| \leq \hat{r}_j$, the cross-section of $\bar{\mathcal{G}}_j$ (in the α -space) is the ball $\mathcal{B}_{\alpha_j}((\hat{r}_j^2 - \|y - y_j\|^2)^{1/2})$ and that of $\mathcal{X}(u_j)$ is the ellipsoid $\mathcal{E}_{c_j(\|y\|)}$ given by

$$\mathcal{E}_{c_j(\|y\|)} := \{\alpha : (\alpha - \alpha_j)'(S - I)(\alpha - \alpha_j) \leq c_j(\|y\|)\}.$$

Thus we must show for all such y that

$$\mathcal{B}_{\alpha_j} \left(\sqrt{\hat{r}_j^2 - \|y - y_j\|^2} \right) \subset \mathcal{E}_{c_j(\|y\|)}.$$

Since these two sets have their centers at α_j , this is equivalent to

$$\hat{r}_j^2 - \|y - y_j\|^2 \leq \frac{c_j(\|y\|)}{\lambda_{\max}(S - I)}. \quad (11)$$

We show this inequality in the following.

Here we fix $y \in \mathcal{M}^\perp$ with $\|y - y_j\| \leq \hat{r}_j$ and let $\beta = \|y\|$. Then

$$\begin{aligned} c_j(\|y\|) &= \alpha_j'(S - I)\alpha_j + \|y\|^2 \\ &\geq \lambda_{\min}(S - I)\|\alpha_j\|^2 + \|y\|^2 \\ &= (\sigma_m - 1)\|\alpha_j\|^2 + \beta^2. \end{aligned}$$

Also let $\beta_j = \|y_j\|$. Then

$$\begin{aligned} \hat{r}_j^2 - \|y - y_j\|^2 &\leq \hat{r}_j^2 - (\|y\| - \|y_j\|)^2 \\ &= \left[\|\bar{q}_j - q_j\| + c_T\|\bar{q}_j\| + d_T\|\tilde{U}_0\alpha_j\| \right]^2 - (\beta - \beta_j)^2 \\ &\leq \left[\|\bar{q}_j - q_j\| + c_T\|\bar{q}_j\| + d_T\left(1 - \frac{1}{\sigma_m}\right)\|\alpha_j\| \right]^2 - (\beta - \beta_j)^2 \\ &\quad \left(\text{by } \|\tilde{U}_0\alpha_j\| \leq \|I - S^{-1}\|\|\alpha_j\| = \left(1 - \frac{1}{\sigma_m}\right)\|\alpha_j\| \right) \\ &\leq \left\{ \|\bar{q}_j - q_j\| + c_T\|\bar{q}_j\| + \sqrt{\left(\frac{\sigma_m - 1}{\sigma_1 - 1} - \frac{1}{\sigma_1}\right) \left[1 - \sigma_1 \left(\frac{\|\bar{q}_j - q_j\| + c_{T_j}\|\bar{q}_j\|}{\|q_j\|}\right)^2\right]} \|\alpha_j\| \right\}^2 \\ &\quad - (\beta - \beta_j)^2 \quad (\text{by the bound on } d_{T_j} \text{ in (10)}). \end{aligned}$$

Using these inequalities and the fact that $\|\alpha_j\|^2 + \beta_j^2 = \|x_j\|^2$, we can obtain

$$\begin{aligned} &c_j(\|y\|) - (\sigma_1 - 1)(\hat{r}_j^2 - \|y - y_j\|^2) \\ &\geq \sigma_1 \left(\beta - \frac{\sigma_1 - 1}{\sigma_1} \beta_j \right)^2 + \sigma_1 \left(\sigma_m - 1 - \frac{\sigma_1 - 1}{\sigma_1} \right) \left(\frac{\|\bar{q}_j - q_j\| + c_{T_j}\|\bar{q}_j\|}{\|q_j\|} \right)^2 \\ &\quad \times \left[\|\alpha_j\| - \|q_j\| \sqrt{\frac{\sigma_1 - 1}{\sigma_1(\sigma_m - 1) - (\sigma_1 - 1)}} \sqrt{\frac{\|q_j\|^2}{\sigma_1(\|\bar{q}_j - q_j\| + c_{T_j}\|\bar{q}_j\|)^2} - 1} \right]^2. \end{aligned}$$

This is nonnegative because it follows from $S \geq 2I$ that $\sigma_m - 1 - (\sigma_1 - 1)/\sigma_1 > 0$. Hence, (11) is shown. ∇

Step 2 For $j \in \mathcal{S}_1$, $\bar{\mathcal{G}}_j \subset \mathcal{B}_0(r_1)$.

Proof Fix $j \in \mathcal{S}_1$ and $x \in \bar{\mathcal{G}}_j$. From (7), clearly

$$\begin{aligned} \|x\| &\leq \|q_j\| + \|\bar{q}_j - q_j\| + c_T\|\bar{q}_j\| + d_T\|u_j\| \\ &\leq \|q_j\| + \|\bar{q}_j - q_j\| + c_T\|\bar{q}_j\| + d_T \left(1 - \frac{1}{\sigma_m}\right) \|\alpha_j\| \quad (\text{by } u_j = \tilde{U}_0\alpha_j) \\ &\leq r_1. \end{aligned}$$

Thus, $x \in \mathcal{B}_0(r_1)$. ▽□

Some remarks are now in order. In our approach, the design problem has been reduced to the condition $\bar{\mathcal{G}}_j \subset \mathcal{X}(u_j) \cup \mathcal{B}_0(r_1)$ for all $j \in \mathcal{S}$. To show this is still a difficult task. Instead, we have resorted to showing $\bar{\mathcal{G}}_j \subset \mathcal{X}(u_j)$ for most of j , and $\bar{\mathcal{G}}_j \subset \mathcal{B}_0(r_1)$ for j in a finite subset \mathcal{S}_1 of \mathcal{S} . The two steps in the proof above correspond to these conditions.

Through Step 4 in the construction of the controller, there is some flexibility in the choice of $T \geq T^*$. This is important since, in our setup, we are concerned with data rate, and hence the design objective is to obtain a large T while T^* may be very small. We note, however, that there is a trade-off between the sizes of T and r_1 , i.e., for larger T , the attractive ball is larger.

This result can be applied to the design of uniform and logarithmic quantizers. Interestingly, for the logarithmic case, the bounds on c_{T_j} become identical and so do those on d_{T_j} . Moreover, asymptotic stability can be achieved, which is never possible by uniform quantizers.

We state the result for the logarithmic case as a corollary for later use. Take $\delta \in (1, (\sqrt{\sigma_1} + 1)/(\sqrt{\sigma_1} - 1))$. Note that $\sigma_1 \geq 2$ by the assumption $S \geq 2I$, so such a δ always exists.

Corollary 4.5 Select $T > 0$ small enough that

$$c_T < \frac{1}{2\delta} \left(\frac{\delta + 1}{\sqrt{\sigma_1}} - \delta + 1 \right), \quad d_T \leq \frac{\sigma_m}{\sigma_m - 1} \sqrt{\left(\frac{\sigma_m - 1}{\sigma_1 - 1} - \frac{1}{\sigma_1} \right) \left[1 - \sigma_1 \left(\frac{(1 + 2c_T)\delta - 1}{\delta + 1} \right)^2 \right]}.$$

Then, the closed-loop system using the logarithmic quantizer with δ and T is quadratically stable with respect to $(P_s, \epsilon J_s)$.

An interesting observation here is that there is an implicit tradeoff between δ and T . These are the key parameters that determine the coarseness and the sampling period, and consequently the communication rate. We also remark that, in this state quantization problem, the choice of the parameter δ is limited by an upper bound. In contrast, such a bound does not exist in the results in [6], where it is the control $Kx(t)$ that is sampled and quantized (instead of $x(t)$).

5 Two-stage design

In this section, the quantizers in the remote control system are designed through two stages.

5.1 Stage 1

The first stage consists of two design problems, one for Q_s and the other for Q_o . The state quantizer Q_s is designed through the state feedback stabilization described in Section 4. We limit the quantizer class to that of logarithmic ones and use Corollary 4.5. For a prespecified decay rate, we obtain the parameter $\delta_s^* > 1$ and the sampling period $T_s^* > 0$. Note that the system remains stable under the same stability criterion for any sampling period smaller than or equal to T_s^* and also for any $\delta_s \in (1, \delta_s^*]$.

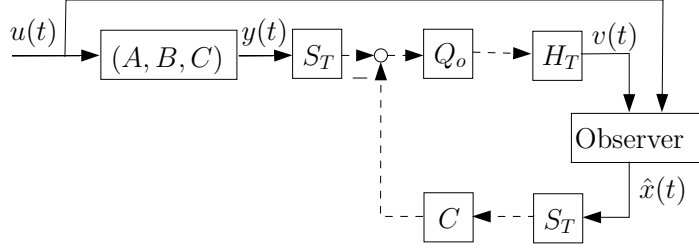


Figure 7: System for output quantizer design

The output quantizer Q_o is designed similarly using the methods in [6]. Here again we use a logarithmic type. We next summarize the design procedure: Consider the system in Fig. 7. The observer has a state equation

$$\dot{\hat{x}}(t) = A\hat{x}(t) + Bu(t) - Lv(t),$$

where $v(t) = Q_o(C\hat{x}(kT) - y(kT))$ for $t \in [kT, (k+1)T)$. Let the error be $e(t) = x(t) - \hat{x}(t)$. The error dynamics is $\dot{e}(t) = Ae(t) + Lv(t)$.

Given $\epsilon_o \in (0, 1)$ and positive-definite matrices W and V , solve the Riccati equation $P_o A' + AP_o - P_o C' V^{-1} C P_o + W = 0$ and obtain the solution P_o . Then let $L \in \mathbb{R}^{n \times p}$ be the optimal estimator gain, $L = -P_o C' V^{-1}$. Pick as the Lyapunov function $V_o(e) = e' P_o e$, and let its time derivative be $\dot{V}_o(e, v) := (Ae + Lv)' P_o e + e' P_o (Ae + Lv)$. Note that with full error feedback, i.e., $v = y - C\hat{x}$, we have $\dot{V}_o(e, v) = -e' J_o e$, where $J_o := W + P_o C' V^{-1} C P_o$.

We design a logarithmic quantizer Q_o so that the closed-loop system is quadratically stable with respect to $(P_o, \epsilon_o J_o)$ and obtain the sampling period $T_o^* > 0$ and the parameter $\delta_o^* > 1$ for the logarithmic partition as in Section 2. Again, the error system remains stable with the same decay rate for any sampling period smaller than or equal to T_o^* and for any $\delta_o \in (1, \delta_o^*]$.

In summary, in this stage, the quantizers Q_s and Q_o are designed for separate stabilization problems under quadratic stability criteria in continuous time.

5.2 Stage 2

In the second stage, the quantizers Q_s and Q_o from the previous stage are tuned so that the closed-loop remote control system in Fig. 3 is stable. Let $T = \min\{T_s^*, T_o^*\}$. The design parameters are now $\delta_s \in (1, \delta_s^*]$ and $\delta_o \in (1, \delta_o^*]$.

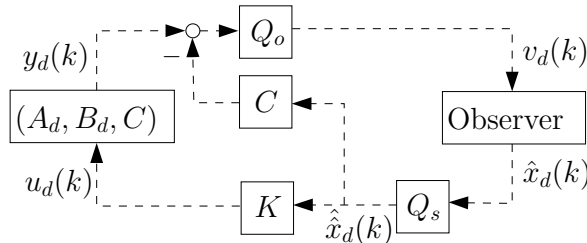


Figure 8: Discrete-time remote control system

This part of the design is carried out in discrete time. The discretized version of the remote control system in Fig. 3 is given in Fig. 8. The signals originally in Fig. 3 correspond to those

with subscripts d in Fig. 8; for example, $y_d(k) = y(kT)$, $k \in \mathbb{Z}_+$. The matrices A, B , and L are discretized to A_d, B_d , and L_d , respectively, as well.

Notice that the plant state equation is now

$$x_d(k+1) = A_d x_d(k) + B_d u_d(k), \quad y_d(k) = C x_d(k),$$

and the control is $u_d(k) = K \hat{x}_d(k)$. Here let the error in state quantization be

$$\hat{e}_d(k) := \hat{x}_d(k) - \hat{\hat{x}}_d(k) = x_d(k) - e_d(k) - Q_s(x_d(k) - e_d(k)). \quad (12)$$

Then, by (1), the observer is expressed as

$$\hat{x}_d(k+1) = A_d \hat{x}_d(k) + B_d u_d(k) - L_d Q_o \left(y_d(k) - C \hat{x}_d(k) \right) + L_d C \hat{e}_d(k).$$

It is straightforward to obtain the following state equations for this system:

$$\begin{aligned} x_d(k+1) &= (A_d + B_d K) x_d(k) - B_d K (e_d(k) + \hat{e}_d(k)), \\ e_d(k+1) &= (A_d + L_d C) e_d(k) + L_d \{ C (e_d(k) + \hat{e}_d(k)) - Q_o [C (e_d(k) + \hat{e}_d(k))] \}. \end{aligned} \quad (13)$$

We make several assumptions. The first one is that a bound on the initial state is known, that is, $\|x(0)\|_\infty \leq \gamma$ for some $\gamma > 0$. The second one is a technical one, made for simplicity: We assume that the matrices $A_d + B_d K$ and $A_d + L_d C$ have only real eigenvalues. The full result for the case of general complex eigenvalues can be found in the appendix.

To deal with the nonlinearity due to the quantizers, we would like to find a linear system whose variables define rectangles that contain the states $x_d(k)$ and $e_d(k)$ at each $k \in \mathbb{Z}_+$. The key observation in deriving such a linear system is that, for logarithmic quantizers, the quantization error is proportional to the input componentwise: For $x \in \mathbb{R}^n$,

$$\left| [x - Q_s(x)]_j \right| \leq \frac{\delta_s - 1}{2} |x_j|, \quad j = 1, 2, \dots, n, \quad (14)$$

where $[\cdot]_j$ denotes the j th component of a vector. We note that this is a tight bound.

We now introduce a change in the coordinates. Let the Jordan canonical forms of the matrices $A_d + B_d K$ and $A_d + L_d C$ be obtained as

$$J_1 = H_1 (A_d + B_d K) H_1^{-1}, \quad J_2 = H_2 (A_d + L_d C) H_2^{-1},$$

respectively, where $H_1, H_2 \in \mathbb{R}^{n \times n}$. Let the new state variables be

$$z_1(k) := H_1 x_d(k), \quad z_2(k) := H_2 e_d(k).$$

For each $i = 1, 2$, let $r_i(k) \in \mathbb{R}_+^n$, and define a rectangle $R_i(k) \subset \mathbb{R}^n$ by

$$R_i(k) := \{ z \in \mathbb{R}^n : |z_j| \leq [r_i(k)]_j, \quad j = 1, 2, \dots, n \}, \quad k \in \mathbb{Z}_+. \quad (15)$$

We would like to find linear state equations for $r_i(k)$ so that $z_i(k) \in R_i(k)$, $i = 1, 2$, for $k \in \mathbb{Z}_+$, and then find conditions such that $r_i(k) \rightarrow 0$ as $k \rightarrow \infty$.

Define an operator on matrices and vectors that takes absolute values of the entries by

$$- : \mathbb{R}^{n_1 \times n_2} \rightarrow \mathbb{R}^{n_1 \times n_2}, \quad \overline{H} = [|h_{ij}|], \quad \text{where } H = [h_{ij}].$$

Using this operator, let

$$\begin{aligned}
A_{r11} &:= \overline{J_1} + \frac{\delta_s - 1}{2} \overline{H_1 B_d K H_1^{-1}}, \\
A_{r12} &:= \overline{H_1 B_d K H_2^{-1}} + \frac{\delta_s - 1}{2} \overline{H_1 B_d K H_2^{-1}}, \\
A_{r21} &:= \frac{\delta_s - 1}{2} \frac{\delta_o - 1}{2} \overline{H_2 L_d C H_1^{-1}}, \\
A_{r22} &:= \overline{J_2} + \frac{\delta_o - 1}{2} \overline{H_2 L_d C H_2^{-1}} + \frac{\delta_s - 1}{2} \frac{\delta_o - 1}{2} \overline{H_2 L_d C H_2^{-1}}.
\end{aligned}$$

Note that the Jordan matrices J_1 and J_2 are Hurwitz and are upper triangular since they have only real eigenvalues by assumption. Hence, $\overline{J_1}$ and $\overline{J_2}$ are Hurwitz as well.

Finally, we describe the linear system of $r_i(k)$, $i = 1, 2$. Let $r_{1j}(0) = \|H_1\|\gamma$ and $r_{2j}(0) = \|H_2\|\gamma$, $j = 1, 2, \dots, n$, and let

$$\begin{bmatrix} r_1(k+1) \\ r_2(k+1) \end{bmatrix} = \begin{bmatrix} A_{r11} & A_{r12} \\ A_{r21} & A_{r22} \end{bmatrix} \begin{bmatrix} r_1(k) \\ r_2(k) \end{bmatrix}. \quad (16)$$

We are now ready to state our solution to the remote control problem.

Theorem 5.1 If $\delta_s, \delta_o > 1$ are small enough so that the matrix in (16) is stable, then the remote control system in Fig. 3 is asymptotically stable. In particular, the linear system (16) of r_1 and r_2 determines the rectangles $R_i(k)$, $i = 1, 2$, in (15) that satisfy $z_i(k) \in R_i(k)$ for all $k \in \mathbb{Z}_+$.

Proof If $z_i(k) \in R_i(k)$ for all $k \in \mathbb{Z}_+$, $i = 1, 2$, and if the system in (16) is stable, then clearly $z_i(k) \rightarrow 0$ as $k \rightarrow \infty$ for $i = 1, 2$. This implies that the discretized remote control system is asymptotically stable and, consequently, that the continuous-time remote control system is asymptotically stable. Hence, we must show $z_i(k) \in R_i(k)$, $i = 1, 2$, for $k \in \mathbb{Z}_+$. This is proved by induction as follows.

By the definition of γ , it is clear that $z_i(0) \in R_i(0)$, $i = 1, 2$. Now suppose $z_i(k) \in R_i(k)$, $i = 1, 2$. Observe that, by (12) and the coordinate change, $\hat{e}_{dj}(k)$, $j = 1, \dots, n$, can be written as

$$\hat{e}_{dj}(k) = [H_1^{-1}z_1(k) - H_2^{-1}z_2(k) - Q_s(H_1^{-1}z_1(k) - H_2^{-1}z_2(k))]_j.$$

Applying inequality (14) to this, we have

$$|\hat{e}_{dj}(k)| \leq \frac{\delta_s - 1}{2} \left| [H_1^{-1}z_1(k) - H_2^{-1}z_2(k)]_j \right|.$$

Then, using the operator $\overline{}$ and the assumption $z_i(k) \in R_i(k)$, we further obtain

$$\begin{aligned}
|\hat{e}_{dj}(k)| &\leq \frac{\delta_s - 1}{2} \left[\overline{H_1^{-1}z_1(k)} + \overline{H_2^{-1}z_2(k)} \right]_j \\
&\leq \frac{\delta_s - 1}{2} \left[\overline{H_1^{-1}r_1(k)} + \overline{H_2^{-1}r_2(k)} \right]_j.
\end{aligned} \quad (17)$$

Next, by (13) and the coordinate change, $z_{1j}(k+1)$, $j = 1, \dots, n$, are expressed as

$$z_{1j}(k+1) = [J_1 z_1(k) - H_1 B_d K (H_2^{-1} z_2(k) + \hat{e}_d(k))]_j.$$

It follows that

$$\begin{aligned}
|z_{1j}(k+1)| &\leq \left| [J_1 z_1(k)]_j \right| + \left| [H_1 B_d K (H_2^{-1} z_2(k) + \hat{e}_d(k))]_j \right| \\
&\leq \left[\overline{J_1 z_1(k)} \right]_j + \left[\overline{H_1 B_d K H_2^{-1} z_2(k)} + \overline{H_1 B_d K \hat{e}_d(k)} \right]_j \\
&\leq \left[\overline{J_1 r_1(k)} \right]_j + \left[\overline{H_1 B_d K H_2^{-1} r_2(k)} + \overline{H_1 B_d K \hat{e}_d(k)} \right]_j.
\end{aligned}$$

By (17), it is clear that the far right hand side above is smaller than or equal to $r_{1j}(k+1)$, given in (16). Hence, $z_1(k+1) \in R_1(k+1)$. Similarly, we can show $z_2(k+1) \in R_2(k+1)$. \square

Denote the A -matrix in (16) by $A_r(\delta_s, \delta_o)$. We have several remarks. First, if $\delta_s = \delta_o = 1$, then the eigenvalues of this matrix are equal to those of $\overline{J_1}$ and $\overline{J_2}$, which are stable. Thus, there always exist $\delta_s, \delta_o > 1$ such that this matrix is stable.

Second, there is a tradeoff between the δ -parameters for $A_r(\delta_s, \delta_o)$ to be stable. We show this in the following. Notice that each element of this matrix is nonnegative; such matrices are called *nonnegative* matrices. For $\delta_s \geq \delta'_s \geq 1$ and $\delta_o \geq \delta'_o \geq 1$, it is clear that $A_r(\delta_s, \delta_o) - A_r(\delta'_s, \delta'_o)$ is nonnegative, and hence it follows from [4, Corollary 8.1.19] that

$$\rho(A_r(\delta_s, \delta_o)) \geq \rho(A_r(\delta'_s, \delta'_o)),$$

where $\rho(\cdot)$ is the spectral radius. This inequality shows that for each fixed $\delta_o > 1$, there is a maximum δ_s (which may be infinity) for the spectral radius to be less than or equal to 1, and vice versa. This implies that increase in one δ may require decrease in the other. We can say in other words that data rate reduction in one direction of communication in Fig. 1 may result in rate increase in the other direction. This tradeoff is an interesting characteristic unique to the remote control setting.

The idea to use a linear system whose states determine rectangles containing states was first proposed in [13], where a setup with one quantizer is studied. There, asymptotic stability is achieved by a quantizer that uses finite data rate but is time varying. In our problem of remote control, by contrast, we use static logarithmic quantizers, driven by our assumption that the computation available on the plant side is limited. As we described in Section 3, there is no matrix multiplication in C_1 and D_2 .

Theorem 5.1 is for global asymptotic stability of the remote control system. With static quantizers, this is not possible without having an infinite number of partition cells. To obtain a result using a finite number of cells, we have to limit the design to trajectories starting in a bounded subset in \mathbb{R}^n and use partition cells that have a finite subset covering this region. Logarithmic quantizers can be modified by taking the union of the cells around axes in Fig. 2. Such analysis should be conceptually straightforward, but may be involved in details.

6 Conclusion

In this paper, we studied the remote control problem, which involves designs of two quantizers in a feedback loop. The class of quantizers is limited to the logarithmic type, and a sufficient condition on quantizer parameters is given. This problem motivated us to extend existing

methods to the state quantization problem. Future research topics on quantization include control with guaranteed performance and distributed control.

References

- [1] R. W. Brockett and D. Liberzon. Quantized feedback stabilization of linear systems. *IEEE Trans. Autom. Control*, 45:1279–1289, 2000.
- [2] N. Elia and S. K. Mitter. Stabilization of linear systems with limited information. *IEEE Trans. Autom. Control*, 46:1384–1400, 2001.
- [3] J. Hespanha, A. Ortega, and L. Vasudevan. Towards the control of linear systems with minimum bit-rate. In *Proc. 15th Int. Symp. MTNS*, 2002.
- [4] R. A. Horn and C. R. Johnson. *Matrix Analysis*. Cambridge University Press, 1985.
- [5] H. Ishii and B. A. Francis. Stabilizing a linear system by switching control and output feedback with dwell time. In *Proc. 40th Conf. on Decision and Control*, pages 191–196, 2001.
- [6] H. Ishii and B. A. Francis. *Limited Data Rate in Control Systems with Networks*, volume 275 of *Lect. Notes Contr. Info. Sci.* Springer, Berlin, 2002.
- [7] H. Ishii and B. A. Francis. Stabilizing a linear system by switching control with dwell time. *IEEE Trans. Autom. Control*, 47:1962–1973, 2002.
- [8] F. L. Lian, J. R. Moyne, and D. M. Tilbury. Performance evaluation of control networks: Ethernet, ControlNet, and DeviceNet. *IEEE Control Systems Magazine*, 21(1):66–83, 2001.
- [9] D. Liberzon. On stabilization of linear systems with limited information. *IEEE Trans. Autom. Control*, 48:304–307, 2003.
- [10] G. N. Nair and R. J. Evans. Stabilization with data-rate-limited feedback: Tightest attainable bounds. *Systems and Control Letters*, 41:49–56, 2000.
- [11] G. N. Nair and R. J. Evans. Exponential stabilisability of finite-dimensional linear systems with limited data rates. *Automatica*, 39:585–593, 2003.
- [12] I. R. Petersen and A. V. Savkin. Multi-rate stabilization of multivariable discrete-time linear systems via a limited capacity communication channel. In *Proc. 40th Conf. on Decision and Control*, pages 304–309, 2001.
- [13] S. Tatikonda. *Control Under Communication Constraints*. PhD thesis, Massachusetts Institute of Technology, Cambridge, MA, 2000.
- [14] W. S. Wong and R. W. Brockett. Systems with finite communication bandwidth constraints II: Stabilization with limited information feedback. *IEEE Trans. Autom. Control*, 44:1049–1053, 1999.

Appendix

In this section, we outline the extension of Theorem 5.1 for the general case when the matrices $A_d + B_d K$ and $A_d + L_d C$ have complex eigenvalues.

We start with the real Jordan canonical forms [4] of the matrices $A_d + B_d K$ and $A_d + L_d C$:

$$J_1 = H_1(A_d + B_d K)H_1^{-1}, \quad J_2 = H_2(A_d + L_d C)H_2^{-1},$$

where $H_1, H_2 \in \mathbb{R}^{n \times n}$. The Jordan matrices $J_i, i = 1, 2$, have diagonal structures as $J_i = \text{diag}(J_{i1}, \dots, J_{il_i})$, where each Jordan block J_{il} corresponds to an eigenvalue λ_{il} of J_i ; if λ_{il} is real, J_{il} takes the form

$$J_{il} = \begin{bmatrix} \lambda_{il} & 1 & & \\ & \ddots & \ddots & \\ & & \ddots & 1 \\ & & & \lambda_{il} \end{bmatrix},$$

and if the eigenvalue is complex, $\lambda_{il} = |\lambda_{il}|(\cos \theta_{il} \pm j \sin \theta_{il})$, it has the form

$$J_{il} = \begin{bmatrix} |\lambda_{il}| \tilde{F}_{il} & I & & \\ & \ddots & \ddots & \\ & & \ddots & I \\ & & & |\lambda_{il}| \tilde{F}_{il} \end{bmatrix},$$

where

$$\tilde{F}_{il} = \begin{bmatrix} \cos \theta_{il} & \sin \theta_{il} \\ -\sin \theta_{il} & \cos \theta_{il} \end{bmatrix}.$$

Now we define the matrix F_{il} that has the same dimension as the corresponding J_{il} by

$$F_{il} := \begin{cases} I & \text{if } \lambda_{il} \text{ is real} \\ \text{diag}(\tilde{F}_{il}, \dots, \tilde{F}_{il}) & \text{else,} \end{cases}$$

and let $F_i := \text{diag}(F_{i1}, \dots, F_{il_i})$. Note that the matrix $F_i^{-1}J_i$ is upper triangular where each diagonal element is real and is either λ_{il} or $|\lambda_{il}|$. Moreover, since J_i is Hurwitz, $F_i^{-1}J_i$ and hence $\overline{F_i^{-1}J_i}$ are Hurwitz. We remark that the use of such matrices F_i for Jordan matrices was introduced in [13].

The new state variables are given by

$$z_1(k) := F_1^{-k} H_1 x_d(k), \quad z_2(k) := F_2^{-k} H_2 e_d(k).$$

As in Section 5, the goal is to find the linear system (16) so that the rectangles $R_i(k)$ in (15), defined by the states $r_i(k)$ of the system, contain $z_i(k)$ for all $k \in \mathbb{Z}_+$.

To obtain a time-invariant system (16), the matrix F_i^{-k} in the definition of $z_i(k)$ above has to be dealt with. For this purpose, define $\hat{F}_i := \text{diag}(\hat{F}_{i1}, \dots, \hat{F}_{il_i})$, where

$$\hat{F}_{il} := \begin{cases} I & \text{if } \lambda_{il} \text{ is real} \\ \text{diag} \left(\begin{bmatrix} 1 & 1 \\ 1 & 1 \end{bmatrix}, \dots, \begin{bmatrix} 1 & 1 \\ 1 & 1 \end{bmatrix} \right) & \text{else.} \end{cases}$$

Noticing that F_i^{-k} is basically rotational, we easily see that \hat{F}_i bounds it in the sense that, for every $k \in \mathbb{Z}$ and $x \in \mathbb{R}^n$,

$$[\overline{F_i^{-k} x}]_j \leq [\hat{F}_i \bar{x}]_j, \quad j = 1, 2, \dots, n.$$

We are in a position to give the system matrices for the system (16). Let

$$\begin{aligned}
A_{r11} &:= \overline{F_1^{-1}J_1} + \frac{\delta_s - 1}{2} \hat{F}_1 \overline{H_1 B_d K H_1^{-1}} \hat{F}_1, \\
A_{r12} &:= \hat{F}_1 \left(\overline{H_1 B_d K H_2^{-1}} + \frac{\delta_s - 1}{2} \overline{H_1 B_d K H_2^{-1}} \right) \hat{F}_2, \\
A_{r21} &:= \frac{\delta_s - 1}{2} \frac{\delta_o - 1}{2} \hat{F}_2 \overline{H_2 L_d C H_1^{-1}} \hat{F}_1, \\
A_{r22} &:= \overline{F_2^{-1}J_2} + \hat{F}_2 \left(\frac{\delta_o - 1}{2} \overline{H_2 L_d C H_2^{-1}} + \frac{\delta_s - 1}{2} \frac{\delta_o - 1}{2} \overline{H_2 L_d C H_2^{-1}} \right) \hat{F}_2.
\end{aligned}$$

Now, Theorem 5.1 can be extended to the general case when the matrices $A_d + B_d K$ and $A_d + L_d C$ have complex eigenvalues. The proof follows similarly, but makes use of the properties of F_i and \hat{F}_i introduced above.